

NASA TECHNICAL NOTE

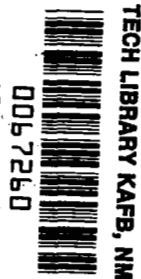
NASA TN D-3294



NASA TN D-3

LOAN COPY: RETUF
AFWL (WLIL-2)
KIRTLAND AFB, N MEX

NASA
CAPE-
ept 3.1
c.1



COLD-AIR PERFORMANCE EVALUATION OF SCALE MODEL OXIDIZER PUMP-DRIVE TURBINE FOR THE M-1 HYDROGEN-OXYGEN ROCKET ENGINE

I - INLET FEEDPIPE-MANIFOLD ASSEMBLY

by Roy G. Stabe, David G. Evans, and Richard J. Roelke

Lewis Research Center

Cleveland, Ohio



NATIONAL AERONAUTICS AND SPACE ADMINISTRATION • WASHINGTON, D. C. • FEBRUARY 1966



0067260

NASA TN D-3294

COLD-AIR PERFORMANCE EVALUATION OF SCALE MODEL
OXIDIZER PUMP-DRIVE TURBINE FOR THE M-1
HYDROGEN-OXYGEN ROCKET ENGINE

I - INLET FEEDPIPE-MANIFOLD ASSEMBLY

By Roy G. Stabe, David G. Evans, and Richard J. Roelke

Lewis Research Center
Cleveland, Ohio

NATIONAL AERONAUTICS AND SPACE ADMINISTRATION

For sale by the Clearinghouse for Federal Scientific and Technical Information
Springfield, Virginia 22151 - Price \$2.00

COLD-AIR PERFORMANCE EVALUATION OF SCALE MODEL
OXIDIZER PUMP-DRIVE TURBINE FOR THE M-1
HYDROGEN-OXYGEN ROCKET ENGINE
I - INLET FEEDPIPE-MANIFOLD ASSEMBLY

by Roy G. Stabe, David G. Evans, and Richard J. Roelke
Lewis Research Center

SUMMARY

A 0.45-scale model of the Model III two-stage oxidizer pump-drive turbine feedpipe-manifold-nozzle assembly for the M-1 1.5-million-pound-thrust hydrogen-oxygen engine was tested with cold air.

The objectives of the tests were to determine flow conditions within the manifold and the overall performance of the feedpipe-manifold assembly. The results of the investigation indicated that a circumferential variation in nozzle-inlet total pressure of 9 percent of feedpipe total pressure existed at approximately design equivalent-inlet total- to nozzle-exit static-pressure ratio. Feedpipe-manifold assembly average total-pressure loss was 5.3 percent of inlet total pressure at design pressure ratio, which corresponds to a loss of 1.06 of the inlet dynamic pressure at a feedpipe Mach number of 0.28. The total-pressure-loss value used in the design, 3.9 percent, was based on an assumed loss of 0.5 of the inlet dynamic pressure for an assumed feedpipe Mach number of 0.35.

At design equivalent-inlet total- to nozzle-exit static-pressure ratio, the measured equivalent weight flow was 10.2 percent less than the design value, of which 3.7 percent was due to a deficit in the scale-model nozzle throat area. The remaining 6.5 percent was attributed to poor flow conditions in the manifold and nozzle channels.

INTRODUCTION

Evaluation of the performance of the pump-drive turbines for the M-1 engine has been included as part of the turbine research and project support programs. The M-1, a

1. 5-million-pound-thrust hydrogen-oxygen rocket engine, utilizes separate fuel and oxidizer turbines driven in series by a gas-generator supply system. The approach used in the design of the turbines was that of compactness, light weight, and reasonable efficiency to reduce engine weight while engine specific-impulse performance was maintained. These considerations led to the use of two-stage velocity-compounded turbines for both fuel and oxidizer pump-drive turbines.

The velocity-compounded type of turbine has always been considered to be sensitive to nozzle performance, as this component must convert virtually all of the available enthalpy to velocity. In turn, the nozzle performance can be strongly influenced by flow conditions upstream of the nozzle. In the M-1 oxidizer turbine, the working fluid was supplied to the nozzle by a system of two feedpipes and a constant-area, toroidally shaped inlet manifold. The manifold was integrated into the turbopump structure to achieve a mechanically compact design. This design resulted in a comparatively small manifold flow area and correspondingly high tangential flow velocities within the manifold. These high velocities at the nozzle inlet can adversely affect nozzle performance and, hence, the performance of the turbine. A detailed investigation was therefore made of the aerodynamic performance of the inlet feedpipe-manifold-nozzle assembly as a part of the oxidizer turbine performance evaluation program. The test unit used was a 0.45-scale model of the Model III two-stage oxidizer pump-drive turbine feedpipe-manifold-nozzle assembly. The tests were performed with air at ambient inlet conditions.

The principal means of investigation were surveys of nozzle-exit total pressure, measurement of weight flow, and measurement of manifold and feedpipe static pressures. The nozzle was not investigated as such but was necessarily a part of the test unit to simulate properly flow conditions within the manifold under operating conditions.

The results are presented in terms of the circumferential variation of nozzle-inlet total pressure, total-pressure loss, manifold static pressures, and weight flow over a range of equivalent-inlet total- to nozzle-exit static-pressure ratios from 1.13 to 1.99. Also included are descriptions of the M-1 turbopump system, test equipment, test facility, and procedures used.

SYMBOLS

A	area, sq in.
D	diameter, in.
g	gravitational constant, 32.17 ft/sec ²
Δh	specific work, Btu/lb
J	mechanical equivalent of heat, 778 ft-lb/Btu

N	rotative speed, rpm
P	turbine power
p	absolute pressure, lb/sq in. abs
q	dynamic pressure, $\left(\frac{\rho V^2}{2g}\right)\left(\frac{1}{144}\right)$, lb/sq in. abs
R	gas constant, ft-lb/(lb)(°R)
r	radius, in.
T	absolute temperature, °R
U	blade speed, ft/sec
V	absolute gas velocity, ft/sec
w	weight flow, lb/sec
γ	ratio of specific heats
δ	ratio of inlet total pressure to NACA standard sea-level pressure, $p'_1/14.696$
ϵ	function of γ used to relate parameters to standard sea-level conditions, $\frac{0.740}{\gamma} \left(\frac{\gamma + 1}{2}\right)^{\gamma/(\gamma-1)}$
η	static efficiency, $\Delta h'/\Delta h_{id}$, based on $p'_1/p_{6,m}$
$\sqrt{\theta}_{cr}$	ratio of critical velocity at inlet total temperature to critical velocity at NACA standard sea-level temperature, $V_{cr,1}/1019.46$
ν	blade-jet speed ratio, $U_m/\sqrt{2gJ\Delta h_{id}}$
ρ	density, lb/cu ft

Subscripts:

a, b	radial-axial cross section in manifold (fig. 1(d))
cr	conditions corresponding to Mach number of 1
eq	equivalent condition
exit	exit station in exhaust pipe, 16.6 in. downstream of station 3 (see fig. 2(a))
h	blade hub section
id	ideal or isentropic
m	blade mean section

max maximum value
 t blade tip section
 1 feedpipe-manifold inlet
 2 manifold
 2c nozzle inlet
 3 nozzle outlet
 6 second-stage rotor outlet

Superscripts:

' total state
 — average value

DESCRIPTION OF M-1 TURBOPUMP SYSTEM

The location of the oxidizer turbopump assembly on the M-1 engine is shown in figure 1(a). The fuel turbopump is located diametrically across the engine from the oxidizer turbopump. The turbines are located at the lower end of each turbopump and are driven by the products of combustion of a fuel-rich hydrogen-oxygen gas generator operating at an oxidant-to-fuel mixture ratio of nominally 0.8.

The combustion products are staged in series through the fuel turbine and then the oxidizer turbine. Twin crossover ducts connect the exhaust housing of the fuel turbine to the inlet manifold of the oxidizer turbine. The ends of the crossover ducts entering the manifold are referred to herein as the "feedpipes." After expanding through the oxidizer turbine, the discharge flow enters a hemispherically shaped exhaust housing from which the two exhaust pipes direct it to the engine skirt manifold, through the skirt coolant passages, and then overboard through choked nozzles around the base of the skirt.

Oxidizer Turbine

Cross-sectional schematic diagrams of the oxidizer turbopump and turbine are shown in figures 1(b) and (c), respectively, with the various components labeled. The oxidizer turbine is a two-stage Curtis type (velocity staged) designed to the specifications listed in tables I to III.

The design distribution of static pressure across each blade row at the mean diameter (33.00 in.) is given in table III.

Further details of the aerodynamic design and performance requirements for the turbine are given in reference 1.

TABLE I. - M-1 OXIDIZER TURBINE

THERMODYNAMIC CONDITIONS

[Hydrogen-oxygen gas.]

Inlet total pressure, p_1' , lb/sq in. abs	208.1
Inlet total temperature, T_1' , $^{\circ}\text{R}$	1190
Oxidant-fuel ratio	0.8
Ratio of specific heats, γ	1.382
Gas constant, R , ft-lb/(lb)($^{\circ}\text{R}$)	425.8

TABLE II. - M-1 OXIDIZER TURBINE DESIGN CONDITIONS

Parameter	Hot-gas hydrogen-oxygen conditions		NACA standard air equivalent conditions		
	Symbol	Full size	Symbol	Full size	0.45 Scale
Mean diameter, in.	D_m	33.00	D_m	33.00	14.85
Turbine power, hp	P	^a 29 120	$\frac{P\epsilon}{\sqrt{\theta_{cr}}\delta}$	485.6	98.33
Weight flow, lb/sec	w	115	$\frac{w\sqrt{\theta_{cr}}\epsilon}{\delta}$	34.92	7.071
Rotative speed, rpm	N	3635	$\frac{N}{\sqrt{\theta_{cr}}}$	852.0	1893
Pressure ratio	$p_1'/p_{6,m}$	1.734	$p_1'/p_{6,m}$	1.742	1.742
Specific work, Btu/lb	$\Delta h'$	179.0	$\frac{\Delta h'}{\theta_{cr}}$	9.832	9.832
Blade-jet speed ratio	ν	0.128	ν	0.128	0.128
Static efficiency	η	0.539	η	0.539	0.539

^aCorrected from that used in ref. 1.

TABLE III. - MEAN DIAMETER DESIGN AXIAL

PRESSURE DISTRIBUTION

Blade row	Pressure, p , lb/sq in. abs		Pressure drop, Δp		Nozzle-inlet total to blade-outlet static-pressure ratio, $p_{2c}'/p_{\text{outlet}}$
	Inlet	Outlet	lb/sq in.	Percent of total	
Nozzle	^a 200.0	126.8	73.2	91.5	1.577
First-stage rotor	126.8	126.8	0	0	1.577
Second-stage stator	126.8	124.8	2	2.5	1.603
Second-stage rotor	124.8	120.0	4.8	6.0	1.667

^aIn design, p_{2c}' assumed equal to p_{2c} .

Oxidizer-Turbine Feedpipe-Manifold-Nozzle Assembly

The aerodynamic features incorporated in the design of the feedpipe-manifold-nozzle assembly of the oxidizer turbine are as follows: The two feedpipes are spaced 80° apart at the point where they enter the manifold, station 1 (fig. 1(d)), to facilitate installation of the turbopump assembly on the engine. The Mach number of the flow at this point in each feedpipe was approximated in the design to be 0.35. The constant cross-sectional area of the manifold in the radial-axial plane (fig. 1(c)) resulted in a variation of the theoretical tangential Mach number around the manifold of from 0.14 and 0.05 at stations a and b, respectively (fig. 1(d)), to zero at the manifold vertical centerline. A flow deflector plate is located in each feedpipe to prevent the flow from impinging directly onto the nozzle tip wall.

In the design, the loss in total pressure between stations 1 and 2c was assumed to equal one-half the dynamic pressure at station 1, that is,

$$p_1' - p_{2c}' = \frac{q_1}{2}$$

For the assumed feedpipe Mach number of 0.35, $(p_1' - p_{2c}')/p_1' = 0.039$. The design total pressure loss was therefore 3.9 percent of the inlet total pressure, which corresponds to a loss total-pressure ratio p_{2c}'/p_1' of 0.961.

It was not the intent of this investigation to evaluate the performance of the nozzle. Including the nozzle as part of the assembly was necessary, however, to establish the correct area ratio and flow distribution within the manifold. The nozzle blading was of conventional subsonic design with cylindrical end walls, a radius ratio r_h/r_t of 0.823, convergent passages, nontwisted constant-section blading, and curved-back suction surfaces downstream of the throat. There are 43 nozzle blades designed to operate at an exit Mach number of 0.80, a leaving angle of 20° from tangential, a total- to static-pressure ratio $p_{2c}'/p_{3,m}'$ of 1.577, and a loss total-pressure ratio p_3'/p_{2c}' of 0.965.

Combining the individual pressure ratios used in the design yields the following overall total- and static-pressure ratios for the complete feedpipe-manifold-nozzle assembly, stations 1 to 3:

$$\frac{p_3'}{p_1'} = \left(\frac{p_{2c}'}{p_1'} \right) \left(\frac{p_3'}{p_{2c}'} \right) = (0.961)(0.965) = 0.927$$

$$\frac{p_1'}{p_{3,m}'} = \left(\frac{p_1'}{p_{2c}'} \right) \left(\frac{p_{2c}'}{p_{3,m}'} \right) = \left(\frac{1}{0.961} \right) (1.577) = 1.640$$

DESCRIPTION OF MODEL PROGRAM

Scale Hardware

The feedpipe-manifold-nozzle assembly for the M-1 oxidizer turbine tested was built to a scale of 0.45 full size to adapt it to an existing cold-air turbine test facility. Because of this adaptation, the unit had a mean nozzle diameter of 14.85 inches. The test unit was designed to operate with cold air instead of the hot hydrogen-oxygen combustion products used in the actual machine.

Schematic diagrams of the scale hardware showing the flow-path geometry and measuring-station locations are shown in figure 2. The differences between the full-size and the scale models may be noted in comparing figure 1(c) with 2(a). Photographs of the hardware are shown in figure 3. Some changes were made to the flow path entering the manifold and the cross-sectional shape of the manifold to simplify fabrication. In so doing, however, the scale cross-sectional area was maintained. Other simplifications, such as the use of standard pipe, led to a reduction in the combined feedpipe area of 1.45 percent from the design value. The right feedpipe contributed two-thirds of the reduction. These minor deviations were considered to have a second-order effect on the performance of the assembly.

The nozzle blading was formed by electrical discharge machining to a surface finish averaging 60 microinches. Deviations from design specification during manufacture resulted in a nozzle throat area averaging 3.7 percent less than design caused by both the blade heights and the channel throat widths being less than design.

Test Apparatus

The test apparatus is shown in figure 4. In operation, air from the laboratory high-pressure, dry-air system flows through a calibrated orifice and an automatic pressure control valve into the test unit through an 8-inch-diameter header connecting the two feedpipes. After passing through the test unit, the air was discharged through the exhaust pipe and exit control valve to the laboratory altitude-exhaust system.

Instrumentation

The circumferential locations of static pressure taps at stations 1, 2, and 3 are shown in figures 5(a), (b), and (c), respectively. There are four static taps, a Kiel-type total-pressure probe, and two thermocouple total-temperature probes in each feedpipe at station 1. Eight static taps are around the periphery of the manifold at station 2. Three

nozzle channels have static taps in the hub and the tip walls 1/16 inch upstream of the nozzle exit at station 3 (fig. 2(b)). The arithmetic average of the pressures measured with these taps $\bar{p}_{3,m}$ is used to determine the equivalent-inlet total- to nozzle-exit static-pressure ratio $p'_1/\bar{p}_{3,m}$. The nozzle blade surface velocity distributions presented in reference 1 indicate that the static pressure at the tap locations is substantially the same as the free-stream static pressure. The exit static pressure was measured by four equally spaced wall static taps in the exhaust adapter, 16.6 inches downstream of station 3 (fig. 2(a)). The exit static pressure was used for test operations only.

The total pressure at the nozzle exit was measured with a small shielded total-pressure probe. The probe was made from 0.020-inch-diameter tubing with a wall thickness of 0.0025 inch. The diameter of the shield was 0.064 inch. The shielded probe, together with a calibrated strain gage absolute pressure transducer, was mounted to the turbine shaft, which was motor driven (figs. 5(d) and (e)). This arrangement permitted circumferential surveys of the nozzle-exit total pressure at any desired radius. The probe element was positioned 1/8 inch downstream of the nozzle trailing edge (see fig. 2) and set at the nozzle leaving angle of 20° from tangential.

The electrical signal output of both the survey probe transducer and the turbine shaft driven potentiometer, which provided an indication of probe circumferential position, was continuously recorded on a two-pen strip-chart recorder.

A calibrated ASME orifice was used to measure weight flow. Orifice inlet pressure was read on a calibrated precision Bourdon tube gage. All other pressures were recorded by photographing a bank of mercury manometers which were connected to the pressure instrumentation described previously. Temperatures were read with a direct reading, self-balancing potentiometer.

Test Procedure

Inlet total pressure was set at 14.7 pounds per square inch absolute and was automatically maintained by the inlet valve controller. Pressure ratios were varied by changing the exhaust-pipe static pressure while the inlet pressure was held constant. Data were taken at equivalent-inlet total- to nozzle-exit static-pressure ratios $p'_1/\bar{p}_{3,m}$ of approximately 1.13, 1.22, 1.48, 1.77, and 1.99. Inlet total temperature T'_1 was approximately 545°R .

After the inlet pressure and pressure ratio had been set and steady-state flow conditions had been established, the nozzle circumferential survey was started, and pressure, temperature, and weight flow data were taken. The probe was traversed circumferentially through an arc of approximately 400° . Probe speed varied from 4.3 to 5.0 inches per minute, depending on probe radial position.

Data Reduction

Manometer column heights were read from the photographic film. These data and the hand-recorded data (temperatures and orifice inlet pressure) were then converted to compatible engineering units and performance parameters calculated with the aid of a digital computer.

The nozzle-exit total-pressure survey data were reduced manually from the strip-chart record. The maximum readings for each channel and each run were tabulated. The maximum value for each channel at the nozzle mean diameter was assumed to be equal to the total pressure at the inlet of the nozzle channel (station 2c). Reference 2 indicates this assumption to be a reasonable one.

No corrections for pressure measurement error due to shock loss were applied to the data obtained from surveys at supercritical pressure ratios for two reasons: (1) The Mach number at the channel centerline could be only slightly greater than 1 with a resulting negligible loss, and (2) corrections could not be applied uniformly because of the large circumferential variations encountered.

The nozzle channels were arbitrarily numbered from 1 to 43 in a counterclockwise direction viewed upstream, with channel 1 to the left of the trailing edge of blade 1, which lies on the vertical centerline (fig. 5(c)).

Inlet total pressure was measured with a Kiel-type total-pressure probe in the center of each feedpipe; however, this measurement was used primarily for test operations. The inlet total pressure used in the data presented herein was calculated from the average inlet static pressure and total temperature of both feedpipes and total weight flow by use of the following equation:

$$p'_1 = \bar{p}_1 \left\{ \frac{1}{2} + \frac{1}{2} \left[1 + \frac{2(\gamma - 1)R}{\gamma g} \left(\frac{w \sqrt{T'_1}}{\bar{p}_1 A_1} \right)^2 \right]^{1/2} \right\}^{\gamma/(\gamma-1)}$$

Equivalent-inlet total- to nozzle-exit static-pressure ratios $p'_1/\bar{p}_{3,m}$ are for air at NACA standard sea-level conditions ($\gamma = 1.4$). The design point equivalent-inlet total- to nozzle-exit static-pressure ratio was calculated as follows:

$$6 \left[1 - \left(\frac{\bar{p}_{3,m}}{p'_1} \right)^{2/7} \right]_{\text{eq}} = \left\{ \frac{\gamma + 1}{\gamma - 1} \left[1 - \left(\frac{p_{3,m}}{p'_1} \right)^{(\gamma-1)/\gamma} \right] \right\}_{\text{H}_2\text{-O}_2}$$

where $p_{3,m}/p_1' = 1/1.640$ and $\gamma = 1.382$ for the hydrogen-oxygen mixture with the resulting $(p_1'/\bar{p}_{3,m})_{eq} = 1.647$.

RESULTS AND DISCUSSION

The principal means used in evaluating the feedpipe-manifold performance were the surveys of nozzle-exit total pressure. Circumferential surveys were made at three radial positions over a range of inlet total- to nozzle-exit static-pressure ratios from 1.13 to 1.99. Measurements of manifold static pressure at eight circumferential locations and weight flow were also recorded. These data are presented for the same range of pressure ratios as the nozzle-exit surveys. Nozzle-exit static radial pressure gradient data are given for one pressure ratio only.

Nozzle-Exit Surveys

A small shielded total-pressure probe mounted just behind the nozzle trailing edge and set at the blade angle was traversed circumferentially through approximately 400° . Pressure and probe position transducer outputs were continuously recorded on a two-pen strip-chart recorder. A typical survey record is shown in figure 6. Blade channels are numbered according to the convention of figure 5(c). The diagonal line (in conjunction with a calibration curve) indicates probe circumferential position. A pressure scale is included in the figure for reference.

The objective of these tests was to evaluate the feedpipe-manifold assembly performance. Accordingly, no attempt was made to integrate the nozzle-exit pressure profiles and calculate from these the nozzle velocity coefficient or efficiency. The maximum pressure recorded at the mean diameter of each channel was assumed to be equal to the total pressure existing at the entrance of the nozzle channel (station 2c; $p_{3,m,max}' = p_{2c}'$), as discussed in the Data Reduction section. The shape of the pressure profiles, however, is of interest and aids in understanding some of the performance characteristics of this type of design. Typical exit total-pressure profiles for several nozzle channels at three equivalent-inlet total- to nozzle-exit static-pressure ratios are reproduced in figure 7. The assumed direction and relative magnitude of the channel inlet flow vector is indicated in the last column. The total-pressure profiles are oriented vertically relative to the inlet total pressure. The amplitudes of the profile traces are proportional to the nozzle-exit total pressure p_3' , and the distance between the maximum pressure of each profile trace and the line designated p_1' is proportional to the feedpipe-manifold total-pressure

loss $p_1^t - p_{2c}^t$. This information is qualitative; nevertheless, several tentative observations may be made:

(1) The amplitudes of the various nozzle channel total-pressure profiles indicate a large circumferential variation in nozzle-inlet total pressure.

(2) High total-pressure losses are evident at the exit of channels 9 and 36, which are immediately adjacent to the feedpipes. This location corresponds to station a in figure 1(d), where tangential velocities within the manifold are high. In general, the total-pressure losses increase and the pressure within the nozzle blade trailing edge wakes decreases as the pressure ratio increases. The maximum pressures (nozzle-inlet total pressure) of the channels opposite the feedpipes (channels 6 and 39), however, are virtually equal to the inlet total pressure at all pressure ratios investigated.

(3) The total-pressure losses vary across the nozzle channels and are consistently higher on the blade suction surfaces. Additional suction surface losses are evident for nozzle channels on the right side of the manifold, where flow incidence at the nozzle inlet is positive (fig. 6). Positive incidence requires greater turning of the flow, and this turning may result in separation on the blade suction surface.

Manifold Total-Pressure Distribution

The envelope of the maximum nozzle mean-diameter exit total pressures obtained from the survey records is assumed to be the circumferential distribution of nozzle-inlet total pressure at station 2c. These data are presented in figure 8 for five of the pressure ratios investigated. The ordinate is the feedpipe-manifold loss total-pressure ratio, p_{2c}^t/p_1^t , and the abscissa is the circumferential location at the nozzle inlet, station 2c.

The curves exhibit the same general shape at each equivalent-inlet total- to nozzle-exit static-pressure ratio and emphasize the variation in total pressure around the manifold circumference. In general, the total-pressure loss increases with pressure ratio. The maximum peak to peak pressure excursion at the mean diameter for pressure ratios near design (1.48 to 1.77) is about 9 percent of inlet total pressure. This maximum variation occurs between channels near a feedpipe centerline and those adjacent to a feedpipe. There are two major pressure peaks, one at each feedpipe. At these locations, the flow enters the manifold radially inward, turns to the axial direction, and flows more or less directly out of the manifold through the nozzle channels opposite the feedpipes, apparently without diffusion and total-pressure loss. The balance of the flow must turn and flow tangentially around the manifold before flowing out through the nozzle channels. The turning process involves a flow acceleration. The portion of the flow which turns tangentially subsequently diffuses in the manifold with a resulting total-pressure loss.

Hub, mean, and tip survey data for an equivalent-inlet total- to nozzle-exit static-pressure ratio of 1.48 are shown in figure 9. The ordinate is the maximum nozzle-channel-exit loss total-pressure ratio $p'_{3, \max}/p'_1$, and the abscissa is the circumferential location at the nozzle exit (station 3).

The nozzle hub and tip section losses are generally higher than the mean section loss. The greatest total-pressure losses occur at the tip section, most noticeably for those nozzle channels near the feedpipes. The high flow velocity in the radial-axial plane at the feedpipe locations apparently results in flow separation at the nozzle tip wall, which causes the large total-pressure losses observed. Nozzle mean and hub section total-pressure losses at the feedpipe regions are very small, as noted in the discussion of figure 8.

Manifold Total-Pressure Loss

Feedpipe-manifold average loss total-pressure ratio p'_{2c}/p'_1 is shown as a function of equivalent-inlet total- to nozzle-exit static-pressure ratio in figure 10(a). The loss total-pressure ratio presented is an arithmetic average of the survey data taken at the mean diameter for all 43 nozzle channels. The overall average total-pressure loss was 5.3 percent of inlet total pressure at the equivalent design pressure ratio of 1.647, compared with the value used in the design of 3.9 percent.

The feedpipe-manifold total-pressure loss, reduced to the ratio of loss to feedpipe dynamic pressure as obtained from weight-flow data, is shown as a function of equivalent pressure ratio in figure 10(b). At the design equivalent pressure ratio of 1.647, the loss in total pressure was 1.06 of the feedpipe dynamic pressure at an experimentally determined feedpipe Mach number of 0.28. The value used in the design was a loss in total pressure of 0.5 of the feedpipe dynamic pressure evaluated at an assumed feedpipe Mach number of 0.35, which resulted in a design total-pressure loss of 3.9 percent of inlet total pressure, as discussed in the Oxidizer-Turbine Feedpipe-Manifold-Nozzle Assembly section.

The feedpipe Mach number assumed in the design is too high, and the assumed fraction of the feedpipe dynamic pressure lost is too low. These errors in assumption tend to offset each other in such a way that the actual total-pressure loss is 36 percent greater than predicted, even though this loss, when expressed in terms of feedpipe dynamic pressure, is more than twice the value determined in the design.

Manifold Static-Pressure Distribution

The ratio of manifold static to inlet total pressure for the range of equivalent pres-

sure ratios investigated is shown as a function of circumferential position in figure 11. The location of the manifold static taps is shown in figures 2(a) and 5(b). The curves retain the same characteristic shape at each of the equivalent-inlet total- to nozzle-exit static-pressure ratios presented, while the general level of manifold static pressure decreases as the pressure ratio increases. There was little change in the manifold static pressure level, however, as the pressure ratio was increased from 1.77 to 1.99, which indicates that the feedpipe-manifold-nozzle assembly was approaching a choked condition.

Large circumferential static pressure gradients exist for each equivalent pressure ratio presented (fig. 11). In all cases, the lowest manifold static pressures measured occurred adjacent to the feedpipes. The lowest total pressures were measured in approximately the same circumferential location as shown in figure 8. Comparison of these total and static pressures would indicate the existence of low velocities in this region of the manifold, which cannot be the case. Not only must the velocity of the flow be greater in this region of the manifold than in any other, but the turning of the flow from the radial to the tangential direction as it enters the manifold from the feedpipe results in an acceleration of the flow and quite possibly flow separation, which result in a loss of effective flow area. These effects contribute to high velocities. The turning of the flow, with the attendant acceleration, requires a local depression of the static pressure at the manifold outer diameter adjacent to the feedpipes; hence, the static pressures measured in this area were low.

The large dynamic component of the total pressure resulting from high manifold tangential velocities adjacent to the feedpipes is not available to the nozzle channels and is lost because of flow incidence at the nozzle inlet. This situation would account for the low total pressures measured in this area. The maximum total pressure measured downstream of the nozzles is considered to be the effective nozzle inlet total pressure available to the nozzle process rather than the true manifold total pressure. The feedpipe-manifold loss total-pressure ratio \bar{p}_{2c}'/p_1' , as presented in figure 10, then includes the nozzle inlet incidence loss as well as the feedpipe-manifold flow losses.

The static pressures throughout the balance of the manifold were comparatively high. The correspondingly low tangential velocities resulted in lower nozzle channel losses as shown in the nozzle-exit total-pressure profiles in figure 7.

Nozzle-Exit Radial Static-Pressure Distribution

The radial distribution of nozzle-exit static pressure (station 3) is shown in figure 12. The curves are for the three nozzle channels provided with hub and tip wall static taps (figs. 2(b) and 5(c)) and at an equivalent-inlet total- to nozzle-exit static-

pressure ratio of 1.48. Also shown is the theoretical static-pressure distribution for constant-angle blading. This distribution was calculated from channel 23 hub static pressure with a constant loss total-pressure ratio p_3^t/p_1^t from hub to tip of 0.96 assumed. The measured radial distribution agrees fairly well with the theoretical value.

Weight Flow

The variation in equivalent weight flow with pressure ratio is presented in figure 13. At design equivalent-inlet total- to nozzle-exit static-pressure ratio, the actual equivalent weight flow $w \sqrt{\theta_{cr}} \epsilon / \delta$ was 10.2 percent less than the indicated design value. Of this amount, 3.7 percent is chargeable to the nozzle-throat-area deficit mentioned previously. The remaining 6.5 percent is attributed to the effect the flow incidence and distortion in the feedpipe-manifold assembly had on the nozzle performance. Figure 13 shows only a gradual increase in equivalent weight flow for pressure ratios above 1.77. Apparently, close to maximum equivalent weight flow was attained at the highest pressure ratio investigated, 1.99, although it is possible that all nozzle channels were either not choked or choked at progressively higher pressure ratios.

SUMMARY OF RESULTS

The results of an experimental investigation performed with cold air on a 0.45-scale model feedpipe-manifold-nozzle assembly for the M-1 engine oxidizer pump-drive turbine are summarized as follows:

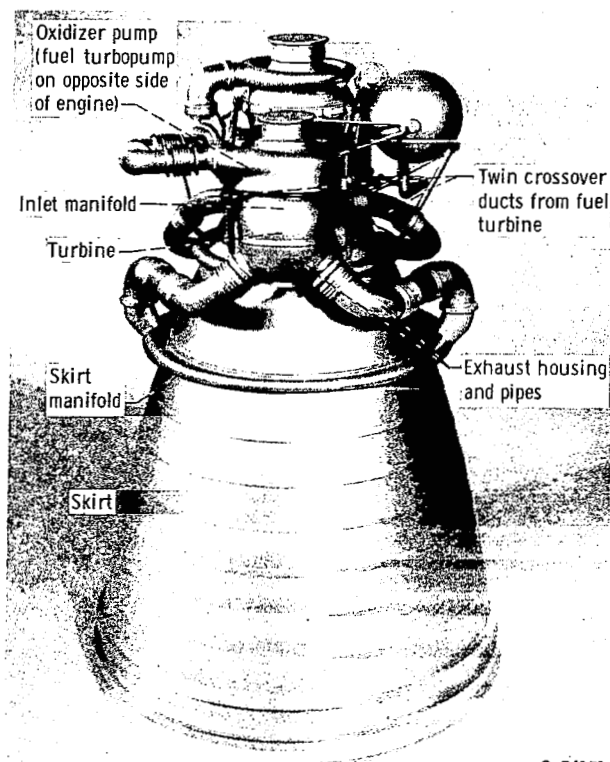
1. Large variations in total and static pressure occurred around the circumference of the manifold. At equivalent-inlet total- to nozzle-exit static-pressure ratios near design, the circumferential variation in nozzle-inlet total pressure was as large as 9 percent of the inlet total pressure.
2. Total-pressure losses chargeable to the feedpipe-manifold assembly averaged 5.3 percent of inlet total pressure at design inlet total- to exit static-pressure ratio, which corresponds to a loss of 1.06 of the feedpipe dynamic pressure at an average feedpipe Mach number of 0.28. The total-pressure-loss value used in the design, 3.9 percent, was based on an assumed loss of 0.5 of the inlet dynamic pressure for an assumed feedpipe Mach number of 0.35.

3. Measured equivalent weight flow was 10.2 percent less than design at the design equivalent-inlet total- to nozzle-exit static-pressure ratio. Part of the discrepancy was due to a 3.7 percent deficit in the scale model hardware nozzle throat area. The balance was attributed to the poor flow conditions existing within the manifold and nozzle channels.

Lewis Research Center,
National Aeronautics and Space Administration,
Cleveland, Ohio, December 2, 1965.

REFERENCES

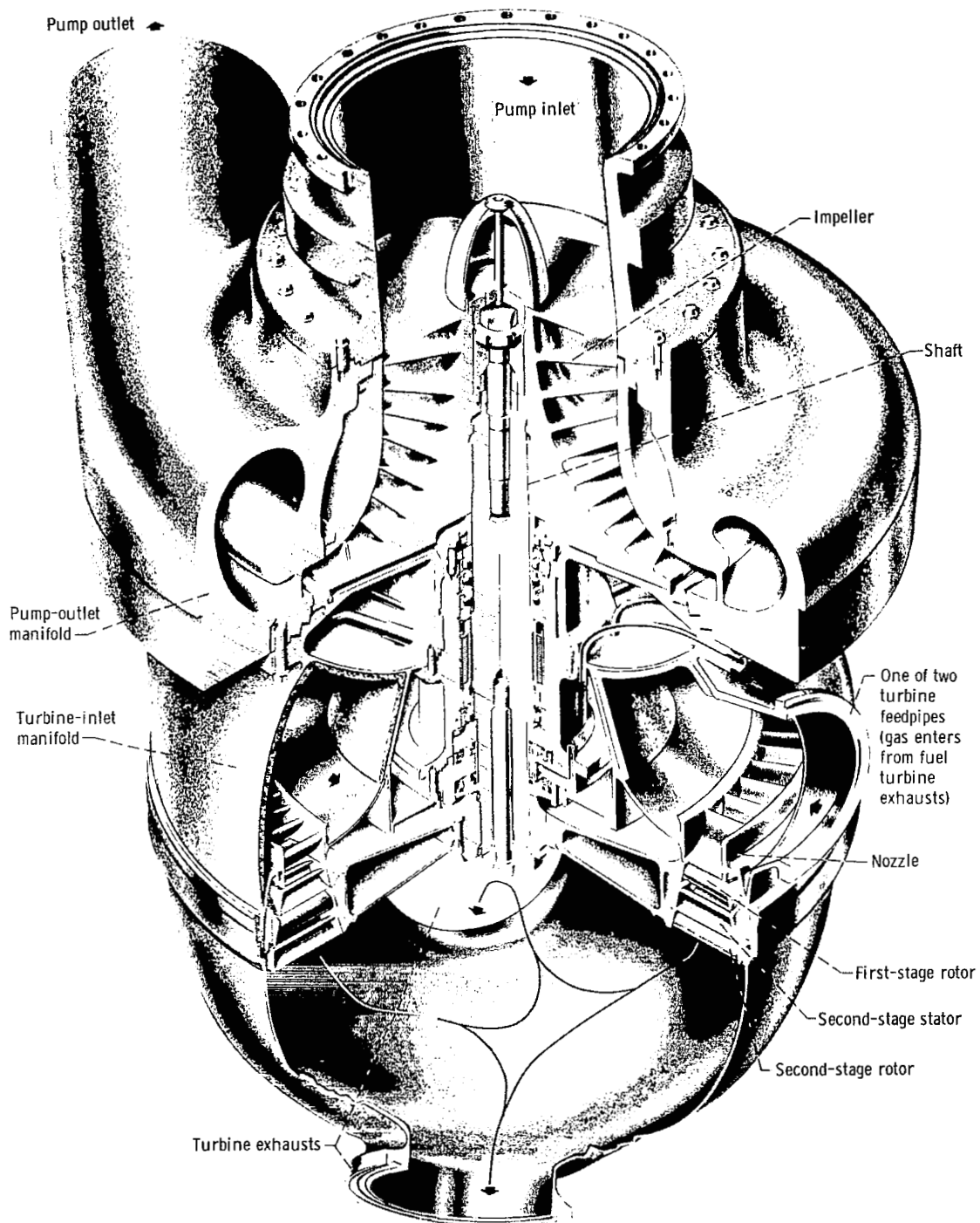
1. Beer, R.: Aerodynamic Design and Estimated Performance of a Two-Stage Curtis Turbine for the Liquid Oxygen Turbopump of the M-1 Engine. NASA CR-54764, 1965.
2. Rohlik, Harold E.; and Kofskey, Milton G.: Secondary-Flow Phenomena in Stator and Rotor-Blade Rows and Their Effect on Turbine Performance. Paper 63-AHGT-72, ASME, Mar. 1963.



C-74171

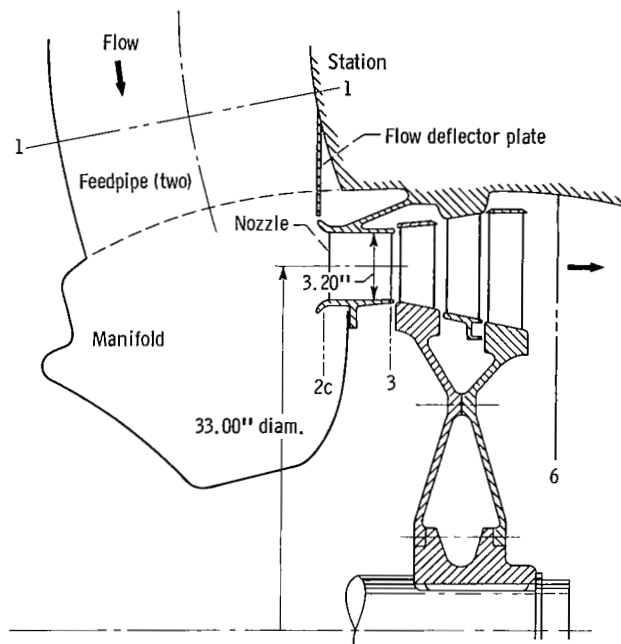
(a) Model of engine.

Figure 1. - M-1 rocket engine.

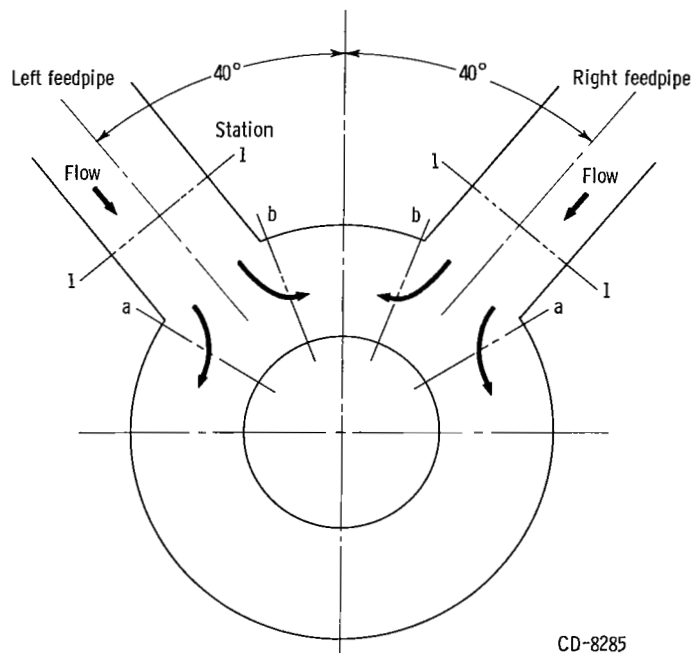


CD-8282

(b) Oxidizer turbopump.
Figure 1. - Continued.



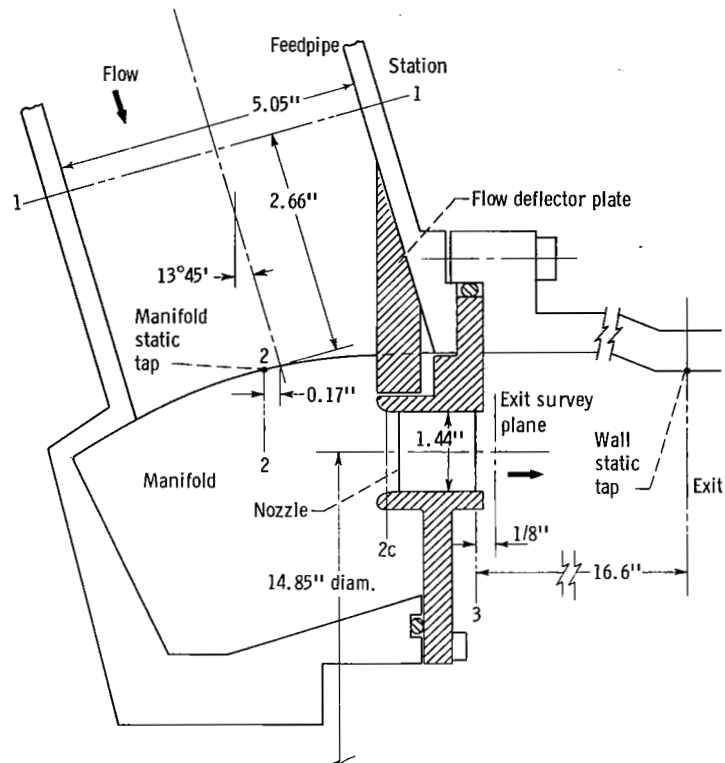
(c) Radial-axial cross section of oxidizer turbine.



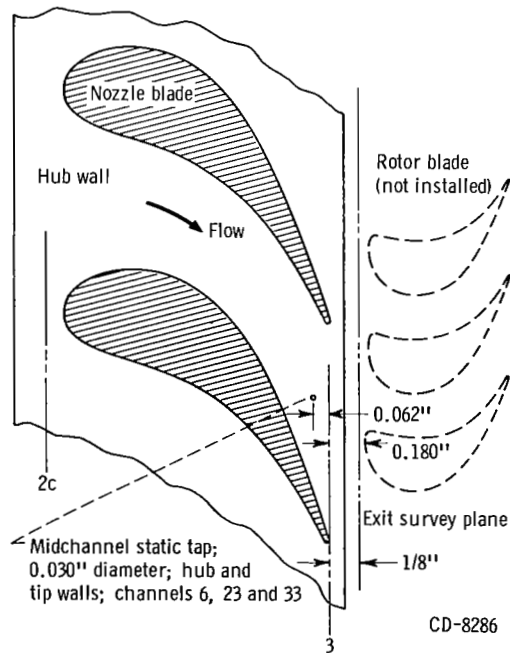
CD-8285

(d) Radial cross section of manifold viewed from station 2c.

Figure 1. - Concluded.



(a) Radial-axial cross section of feedpipe-manifold-nozzle assembly.

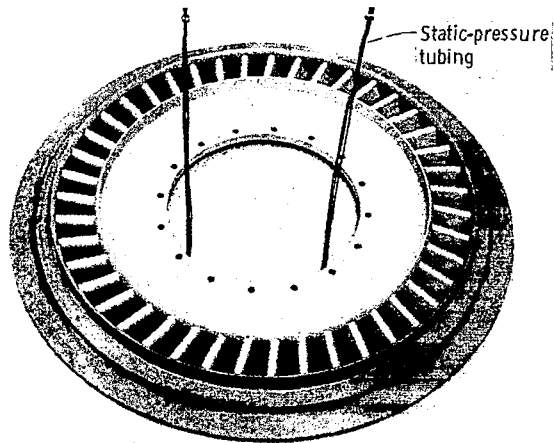


(b) Profile of nozzle blades.

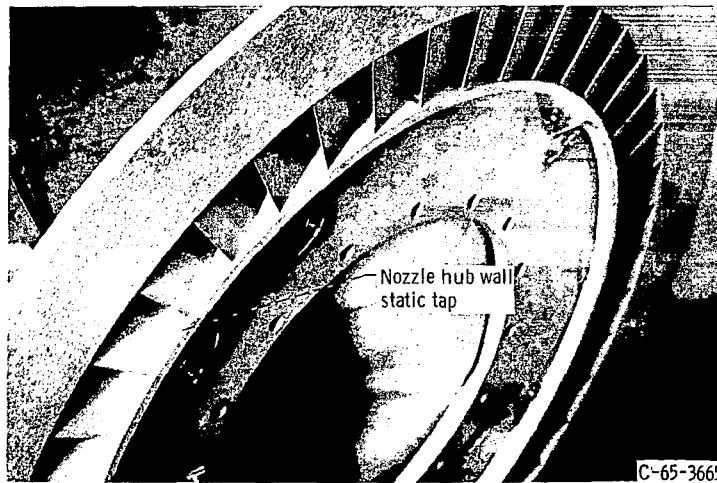
Figure 2. - Flow path and instrument stations of scale model.



(a) Feedpipe-manifold assembly.



(b) Nozzle assembly viewed downstream.



(c) Closeup of nozzle assembly viewed upstream.

Figure 3. - Scale models of feedpipe-manifold and nozzle assemblies.

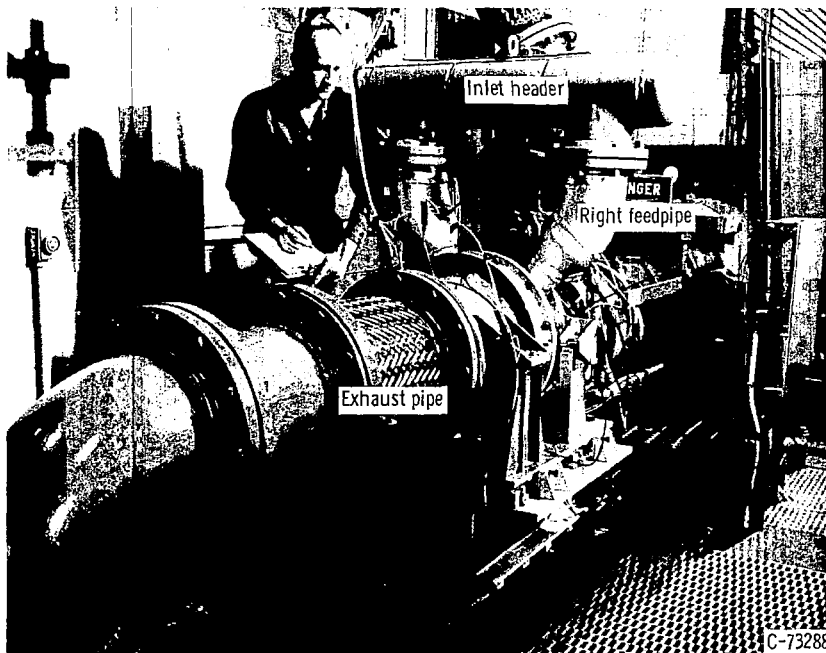
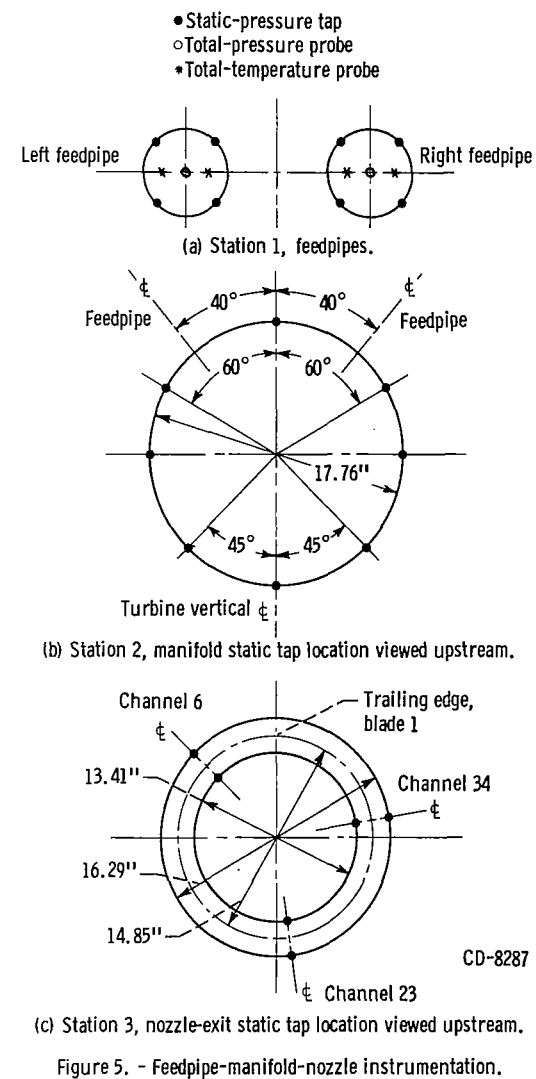
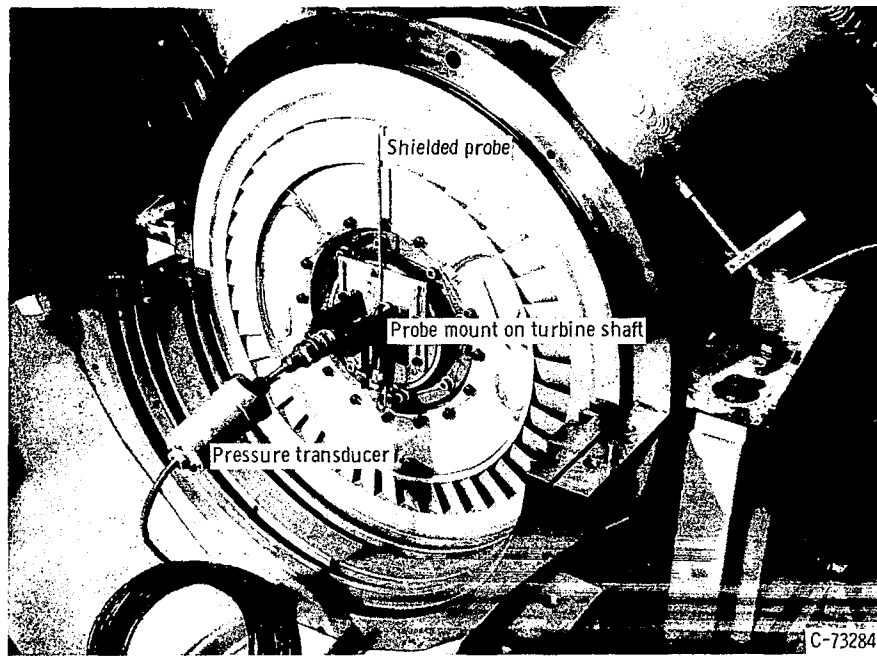
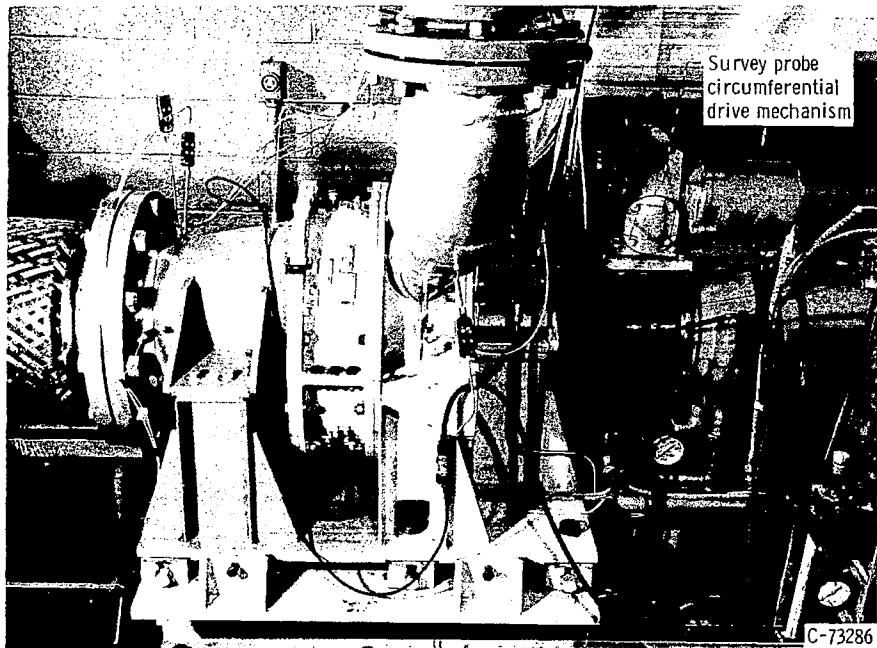


Figure 4. - Overall view of test facility.





(d) Feedpipe-manifold-nozzle assembly with probe, probe mount, and absolute pressure transducer.



(e) Test unit with probe-drive mechanism mounted.

Figure 5. - Concluded.

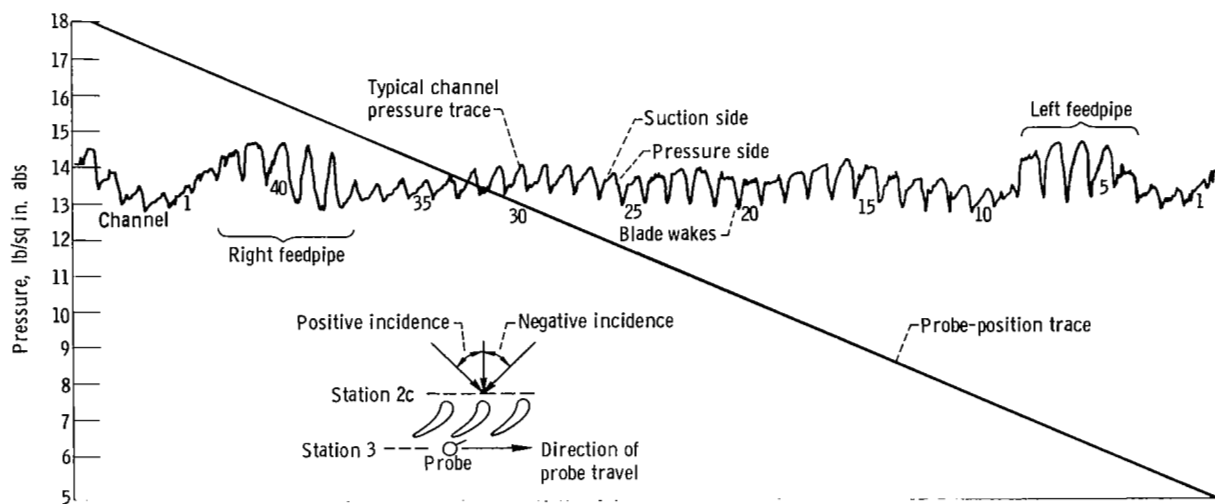


Figure 6. - Strip-chart record of typical nozzle circumferential survey of total pressure at mean diameter, station 3. Equivalent-inlet total- to nozzle-exit static-pressure ratio, 1.48; inlet feedpipe pressure, 14.65 pounds per square inch absolute.

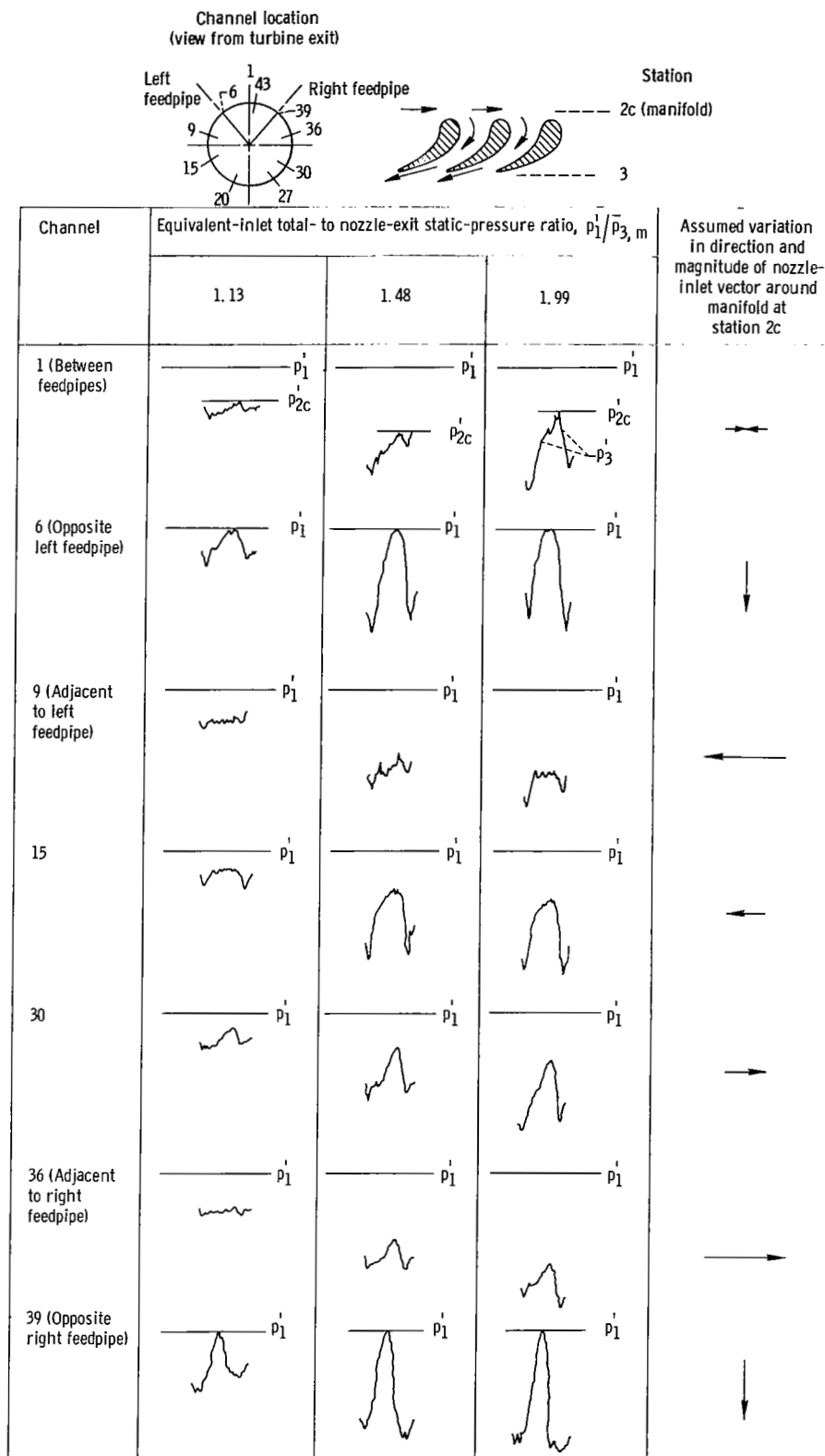


Figure 7. - Mean-diameter nozzle-exit total-pressure profiles for seven nozzle channels and three pressure ratios.

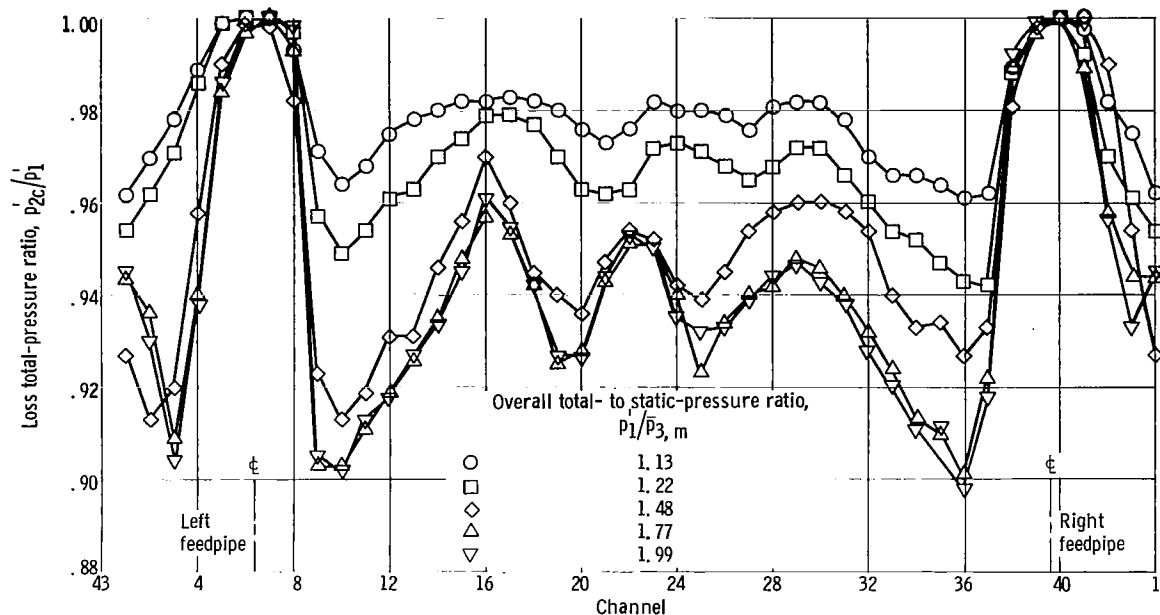


Figure 8. - Circumferential variation of nozzle-inlet total pressure at mean diameter for range of pressure ratios.

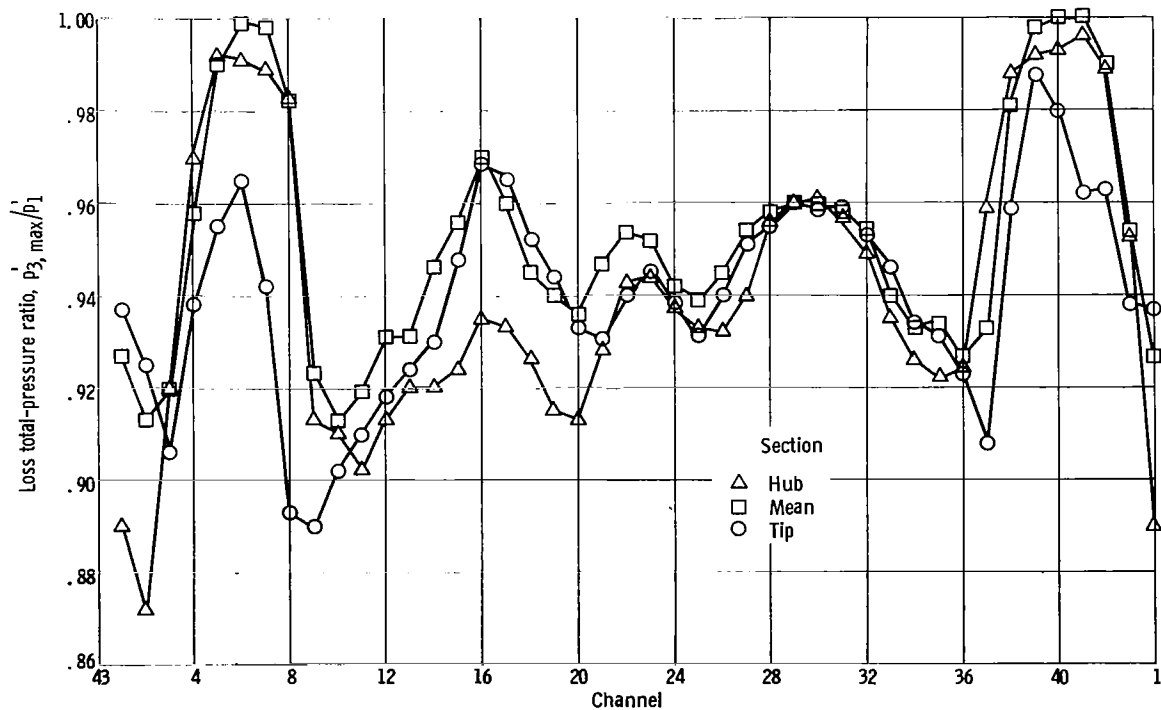
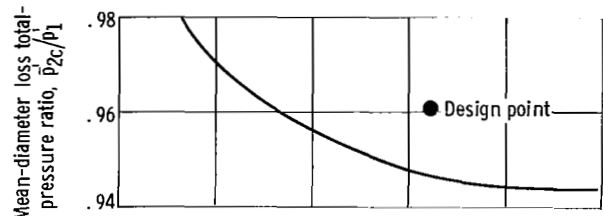
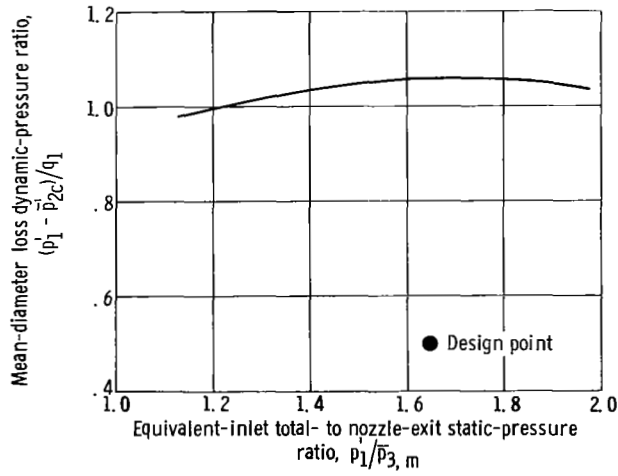


Figure 9. - Circumferential variation of maximum nozzle-exit total pressure at hub, mean, and tip sections for pressure ratio of 1.48.



(a) Average mean-diameter loss total pressure.



(b) Average mean-diameter loss dynamic pressure.

Figure 10. - Feedpipe-manifold total-pressure loss.

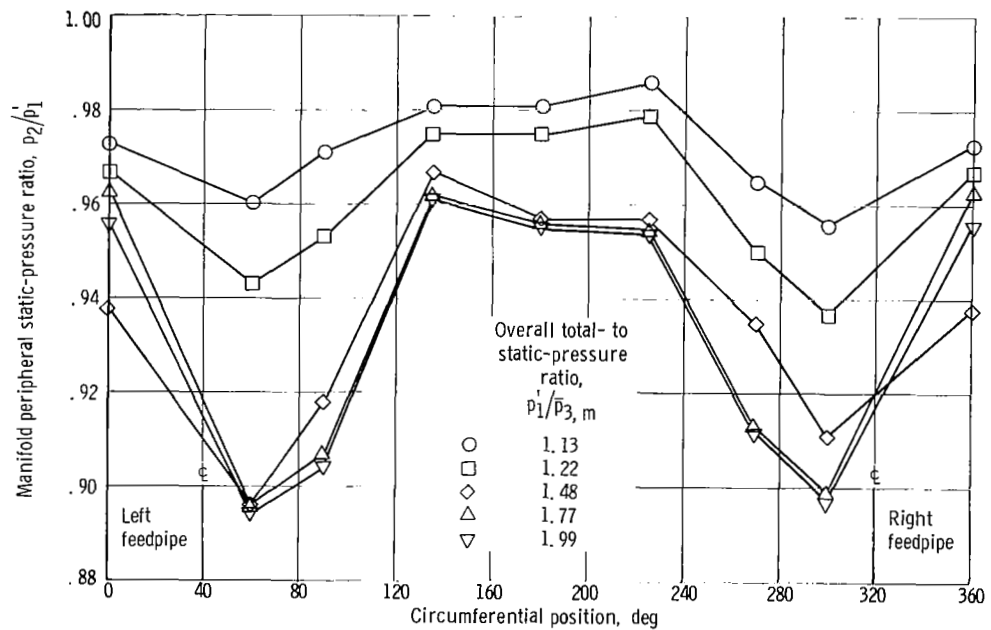


Figure 11. - Circumferential variation of manifold peripheral static pressure.

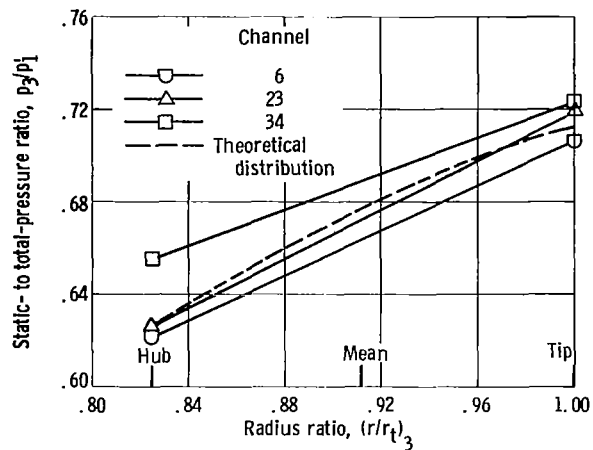


Figure 12. - Nozzle-exit radial static-pressure distribution. Equivalent-inlet total- to nozzle-exit static-pressure ratio, 1.48.

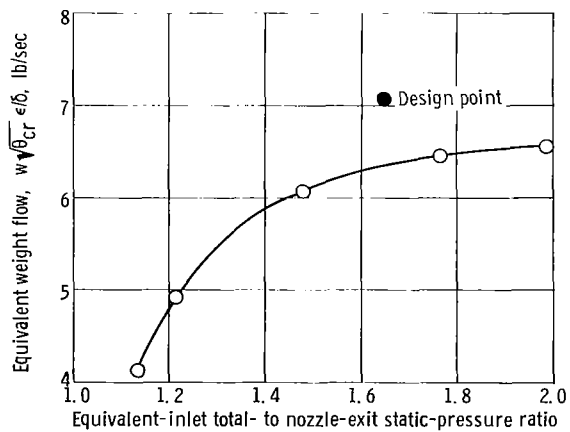


Figure 13. - Scale model feedpipe-manifold-nozzle assembly equivalent weight flow over range of pressure ratios.

"The aeronautical and space activities of the United States shall be conducted so as to contribute . . . to the expansion of human knowledge of phenomena in the atmosphere and space. The Administration shall provide for the widest practicable and appropriate dissemination of information concerning its activities and the results thereof."

—NATIONAL AERONAUTICS AND SPACE ACT OF 1958

NASA SCIENTIFIC AND TECHNICAL PUBLICATIONS

TECHNICAL REPORTS: Scientific and technical information considered important, complete, and a lasting contribution to existing knowledge.

TECHNICAL NOTES: Information less broad in scope but nevertheless of importance as a contribution to existing knowledge.

TECHNICAL MEMORANDUMS: Information receiving limited distribution because of preliminary data, security classification, or other reasons.

CONTRACTOR REPORTS: Technical information generated in connection with a NASA contract or grant and released under NASA auspices.

TECHNICAL TRANSLATIONS: Information published in a foreign language considered to merit NASA distribution in English.

TECHNICAL REPRINTS: Information derived from NASA activities and initially published in the form of journal articles.

SPECIAL PUBLICATIONS: Information derived from or of value to NASA activities but not necessarily reporting the results of individual NASA-programmed scientific efforts. Publications include conference proceedings, monographs, data compilations, handbooks, sourcebooks, and special bibliographies.

Details on the availability of these publications may be obtained from:

SCIENTIFIC AND TECHNICAL INFORMATION DIVISION
NATIONAL AERONAUTICS AND SPACE ADMINISTRATION

Washington, D.C. 20546